SECOND EUROPEAN CONFERENCE ON EARTHQUAKE ENGINEERING
AND SEISMOLOGY, ISTANBUL AUG. 25-29, 2014

STABILITY ANALYSIS OF A ROCK MASS AND EFFECT OF WATER UNDER SEISMIC CONDITIONS: REAL CASE STUDY IN LEBANON

Mirvat ABDALLAH[1,2,3] , Issam SHAHROUR[2] Fadi HAGECHEHADE[3,4]

ABSTRACT

Our scope of work is to analyze the rock slopes stability under seismic conditions with a real Lebanese case study. In engineering practice, most common methods are used to assess the seismic stability of slope consists on a pseudo static approach or traditional approaches based on the limit equilibrium or on the hypothesis of failure calculation. These methods are widely used because of their simplicity but it neglect important elements such as the spatial and temporal variability of the loading, the presence of water, the presence of discontinuities inside the rock in all directions, the influence of reinforcement elements on the stability, …

In this paper, we present a global numerical study of rock slopes stability by using UDEC (Universal Distinct Element Code) software. We consider the case of a slope located in Jezzine (South of Lebanon) under real earthquake records (Kocaeli, 1999). The effect of different configurations of fracture networks is highlighted. In the absence of discontinuities, the rock mass is stable without the registration of permanent displacement in the upper part and it behaves as in the case of the rigid block. The presence of horizontal discontinuities leads to a permanent shift in the upper part of the rock, this shift tends to increase going towards the inside of the model; A small rocking motion induced in the solid by the seismic loading and could be neglected. The presence of horizontal and vertical discontinuities leads to instability of the slope and a rocking motion induced in the solid by the seismic loading and falling of the upper block of the slope.

And in this paper, we present a numerical analysis of the influence of presence of water on the seismic stability of fractured rock slopes. The effect of water flowing on the stability is highlighted.

INTRODUCTION

Lebanon is characterized by its high urbanized mountains and steep slopes. The major structures are Mount Lebanon and the Anti-Lebanon. In general, Lebanese mountains are formed by old rocks formations varying from sedimentary rocks to limestone, dolomite and volcanic ashes. Unfortunately, due to huge demographic expansion and land development even major steep slopes were populated. The absence of a public policy of controlled urbanization, new construction settles in precarious sites, often vulnerable to natural disasters especially in active seismic zone and in poor regions.

From geological point of view, Lebanon contains one major fault and few secondary faults where some ones have been discovered recently. Severe earthquakes could then lead to great human and material losses. In the past, several destructive earthquakes have been occurred in Lebanon for

[1] Currently, Rafik Hariri University, Civil and Environmental Department, Mechref, Damour, Lebanon abdallahma@rhu.edu.lb
[2] Lille 1 University, Laboratory of Civil Enfineering and geo-Environmental LGCgE, Lille, France
[3] Lebanese University, Doctoral School of Science and Technology (EDST), Beirut, Lebanon
[4] Lebanese University, University Institute of Technology, Saida, Lebanon

example in years 551, 1202, 1759, 1837 and 1956. Recently, many earthquakes, of low magnitudes between three and five, have been registered in Lebanon during 2008. These events have increased the anxiety of Lebanese people because of the poor quality of the constructions and their behavior under moderate or severe earthquake events. The efficient way to minimize seismic effects, material and human losses, still the prevention that could be deduced from a better comprehension of the behavior of slopes during and immediately after the seismic events. Given the high seismic risk, it seems necessary to conduct stability analysis of rock masses encountered in the Lebanese mountains.

Generally a discontinuous rock mass deforms preferentially by slipping on preexisting fractures. This movement may be accompanied by an extension of existing fractures and the creation of new fractures. Tracking and morphology of a fracture after brittle deformation are strongly influenced by the texture of the material, the nature of minerals and orientation of microscopic discontinuities with respect to the direction of propagation. The observation of a natural fracture in a granite sample showed that biotite, regardless of size, is systematically fractured and fracturing borrows their differences [Gentier S.].

The seismic loading propagates in the ground by different types of waves. It induces deformations and stresses in the soil. In the presence of water, it may induce a variation of pore pressure, which leads to a variation of the effective stresses of contact and in some cases a reduction of the resistance of geo-materials. Crossing of fractured rock masses, seismic waves generally induce shear stresses at the discontinuity lines, which can cause slippage between the blocs and eventually instability of the rock mass. The vulnerability of a rock to seismic loading depends on many factors, including the magnitude of the seismic acceleration, the duration of the earthquake, the strength characteristics of the mass and dimensions [Abramson L.W. et al.].

Fractures in rock masses can be filled with water or will be the seat of a hydraulic flow. The water in the discontinuities may result from the presence of discontinuities under the groundwater or the water flow during rain or spills of different origins.

The presence of water in the discontinuities has a direct effect on the effective stress, as the water pressure reduces the effective normal stress in the joint, which results in a reduction in the shear strength of the friction joint [Morgenster N.R.].

The seismic loading of fractured rock filled with water induces a change in the water pressure and flow. This change is related to the permeability of joints, hydraulic conditions of joints, magnitude and frequency content of the load. In joints with low permeability and a "fast" loading, seismic loading can induce significant water pressures that can threaten the stability of the rock mass.

The purpose of this work is to analyze the seismic response of fractured rock mass slope corresponding to a real case in Jezzine, South of Lebanon and to analyze the influence of water on the behavior of this rock mass. We perform a numerical modeling by using the UDEC code. We present successively the numerical approach adopted in the UDEC, the case study (geometry, properties, loading ...) and the obtained results by taking different networks of fractures. These studies have shown the importance of taking into account the presence of water in the stability analysis of fractured rock masses affected by water. In this paper, we will conduct a thorough analysis of this problem by using an advanced numerical modeling using the UDEC code to handle the hydro-mechanical coupling in fractured rock under static and dynamic loading. Similar problems have been studied by Jiao et al. 2005, Fischer et al. 2010, Sonmez et al. 2000.

Presentation of Numerical Model

The numerical method falls within the general classification of discontinuum analysis techniques. This approach can represent the geometry of joints and their behavior and to represent the large displacements as well as large deformations. In this work, we utilized the software UDEC (Universal Distinct Element Code) developed by «ITASCA Consulting Group». The domain is represented by an assemblage of discrete blocks. The discontinuities are treated as boundary conditions between blocks; large displacements along discontinuities and rotations of blocks are allowed.

Blocks in UDEC can be either rigid or deformable. Deformable blocks are subdivided into a mesh of finite-difference elements, and each element responds according to a prescribed linear or nonlinear

stress-strain law. The relative motion of blocs is governed by nonlinear force-displacement. UDEC is based on a "Lagrangian" calculation scheme that is well-suited to model the large transformations.

The dynamic analysis is represented numerically by a time-stepping algorithm in which the size of the time-step is limited by the assumption that velocities and accelerations are constant within the time-step. The time-step restriction applies to both contacts and blocks.

The mesh imposes a finite extension of the field. It is necessary to reduce reflections «artificial» of energy to the boundary of the model. A first solution is to remove significantly the limits of the model from the area of interest. This solution leads to make meshes large sizes, which results in a considerable increase in computation time and memory storage required for results. UDEC offers another alternative by applying, at the lateral boundaries, absorbing boundary conditions of type "Quiet Boundaries" or "Free-Field" [Itasca, 2000]. Conditions such as "Quiet Boundaries" simulate free-field motion that would occur in a semi-infinite solid.

Description of the case study

Site Description

The rock covered in this paper is located in Jezzine and which lies 40 km south of Beirut and at an average altitude of 950 m. The data about this were collected from different sources, including field visits, consultation of Google Earth, an analysis of the geological map from CNRS-Lebanon (National Council for Scientific Research) and discussions with professionals who have worked on the site or on adjacent sites. The site and the rock mass are shown in Figure 1. The rock mass consists in a 16m high cliff. The fractures are visible on the mountains; especially we can observe the horizontal and vertical discontinuities.

Figure 1: Site of Jezzine in South Lebanon- view of the cliff

Mechanical properties

The rock mass is formed of sandstone. The morphology of the slope has been strongly affected by erosion processes that have produced cavities and voids of a various sizes. The combined effects of this erosion, the washing out of sand and silt, and the presence of discontinuities leads to rock toppling and rock falls.

The characteristics of the rock mass are summarized in Table 1: we have a soft rock with a Young's modulus of 6 GPa and a Poisson's ratio of 0.25.

Table 1: Mechanical characteristics of the rock mass (Sandstone).

Parameters		Sandstone
Deformation Modulus	E (GPa)	6
Unit weight	γ (KN/m^3)	24.7
Poisson's ratio	Γ	0.25

The mechanical parameters of discontinuities are summarized in Table 2. The normal stiffness is taken equal to the modulus of deformation of the rock. The tangential modulus is equal to half the

normal module. The values attributed to the cohesion and of the friction angle are influenced by the filling and cementing of the joints. The tensile strength is neglected.

Table 2: Mechanical parameters of horizontal and vertical discontinuities.

Parameters		Horizontal discontinuities	Vertical discontinuities
Normal Stiffness	K_n(MPa/m)	$6x10^3$	$6x10^3$
Shear Stiffness	K_s(MPa/m)	$3x10^3$	$3x10^3$
Cohesion	c (MPa)	0.02	0.02
Friction Angle	ϕ (°)	28	0
Tensile Strength	σ_t (MPa)	0	0.1

Mechanical damping is used in the distinct element. The approach is conceptually similar to dynamic relaxation, proposed by Otter et al.. The equations of motion are damped to reach a force equilibrium state as quickly as possible under the applied initial and boundary conditions.

Seismic loading

Due to lacking of seismic records in the site, we have adopted for the seismic loading the data related to the Kocaeli earthquake occurred August 17, 1999 in Turkey. Figures 2-a and 2-b respectively give the variation of the horizontal component of the velocity and its spectrum. We note that the duration of the earthquake is about 30s with a maximum speed of about 40 cm/s (reached after 5 seconds). The velocity spectrum shows that the loading frequency is mainly concentrated between 0 and 2Hz with a major peak at 0.9 Hz. The effect of the vertical component is neglected.

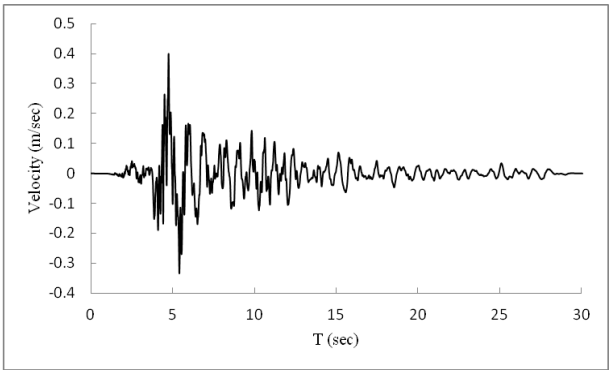

Figure 2-a: Horizontal component of seismic action (Kocaeli – 1999)

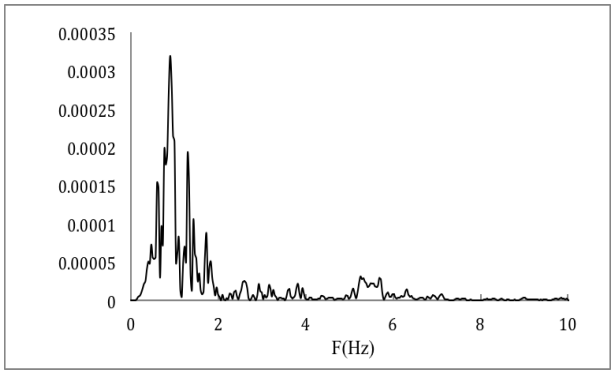

Figure 2-b: Power Spectrum of the horizontal components of the seismic action (Kocaeli-1999)

Analysis of the seismic behavior of the rock mass (without discontinuities)

In this section, we present an analysis of the seismic behavior of the rock mass without discontinuities. This step allows us to define the reference case used later for comparisons.

Figure 3 shows the area considered in the modeling with the horizontal discontinuities. Strong cohesion has been attributed to these discontinuities conditions to ensure perfect contact between the blocks. This figure also defines the position of the points (A, B, C, D, E and F) that will serve as reference points in our interpretation of the seismic response of the massif.

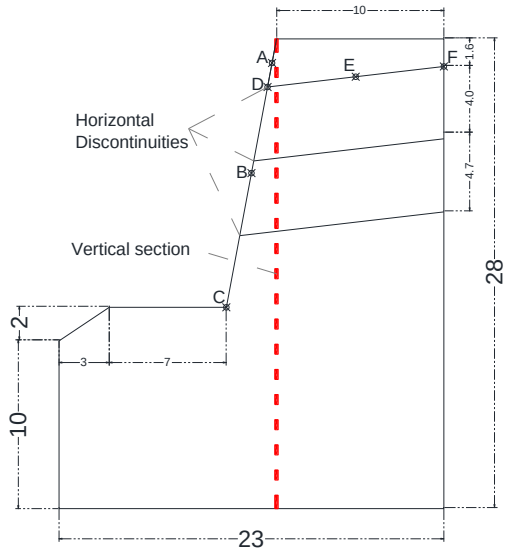

Figure 3: Domain considered in the modeling of the rock mass in jezzine

Initial state - static calculation

In a first step, a static calculation was performed to determine the initial constraints due to the weight of the mass. Figure 4 shows the displacements obtained. We note that these movements are directed downwards (settlement) resulting from the application of its own weight. These displacements are small (less than 1.5 mm), which indicates a good stability of the rock mass under its own weight.

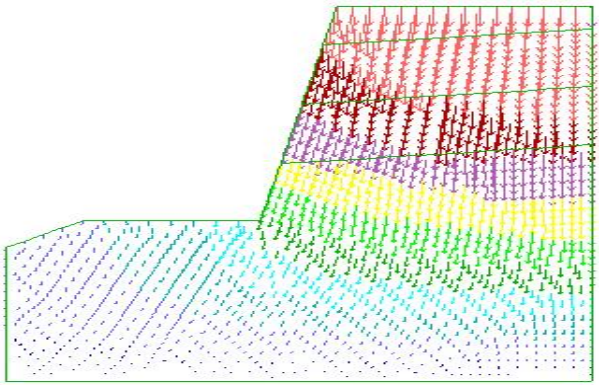

Figure 4: Initial displacement of the rock mass (due to own weight only)

Seismic Analysis

The calculation was carried out by applying the data of the Kocaeli earthquake (Figure 2-a) at the base of the rock. Boundary conditions of type "quiet boundary" imposed on the lateral boundaries of the domain.

Figure 5 shows the horizontal displacements at points A, B and C induced by seismic loading. We note that these movements have the same shape as the imposed loading (Figure 2-a). A maximum displacement of about 6 cm occurs when the seismic loading reaches its peak (at time t = 5 s). We note the following attenuation of lateral displacement to cancel at the end of seismic loading. We can conclude that there is no permanent displacement at the end of loading.

Figure 6 shows the profile of the lateral displacement along a vertical section. There is a movement almost constant with depth, indicating that at the beginning of the loading mass undergoes a motion block with a lateral translation. A slight deformation appears at t = 5 s (peak load speed). Note the

almost cancellation of lateral displacement at the end of loading (t = 25 s). In the absence of discontinuities, the rock behaves as in the case of a rigid block.

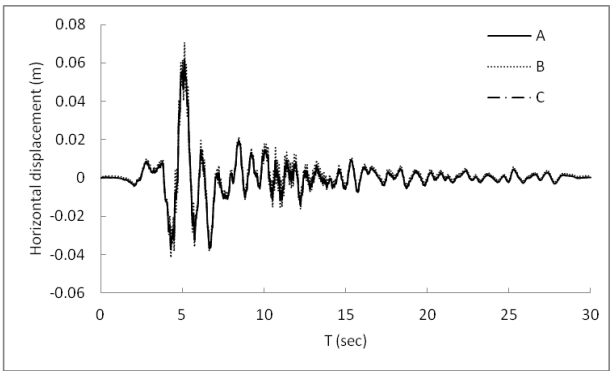

Figure 5: Horizontal displacement induced by seismic loading at three points of the rock mass (Rock mass without discontinuities)

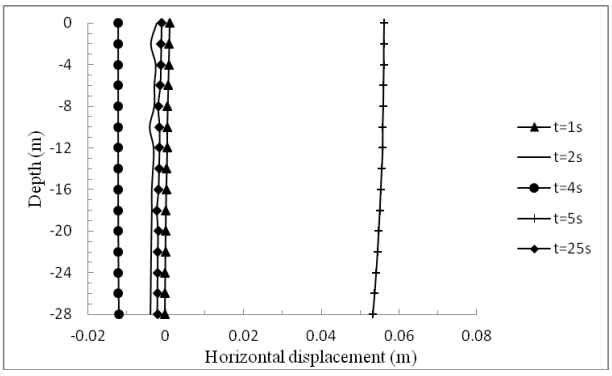

Figure 6: Lateral displacement along the vertical section of the rock mass (rock mass without discontinuities)

Analysis of the seismic behavior of the rock mass - network of horizontal fractures

In this section, analyzes are performed considering the network of horizontal discontinuities (slight slope of 6.6 °). Three lines of discontinuities are considered in the calculation (Figure 3) with the mechanical properties given in Table 2.

Initial state - static calculation

A static calculation was performed to determine the initial constraints due to the weight of the mass. The displacement field obtained is close to that obtained in the previous case (Figure 4). Displacements obtained are small and rock mass is stable under the action of its own weight.

Seismic Analysis

Figure 7-a shows the induced horizontal displacements at points A, B and C of the cliff. At the beginning of loading, the displacements are identical in the three points. The maximum value of 6 cm is obtained 6cm at t = 5. Then, shapes are significantly different with a significant gap between the point C (at the foot of the cliff) and points A and B (at the top of the cliff). At the end of the load, there is a return from the point C to its initial position and a permanent displacement of 5 cm and at point B and 6 cm at point A. Such a trend shows that the seismic loading induced, in the presence of horizontal discontinuities, permanent sliding in the upper part of the rock.

Figure 7-b shows the variation of horizontal displacement along the top discontinuity (DEF). We can note the presence of a permanent displacement along the discontinuity tends to increase when moving from point D to point F (inward massif, Figure 3).

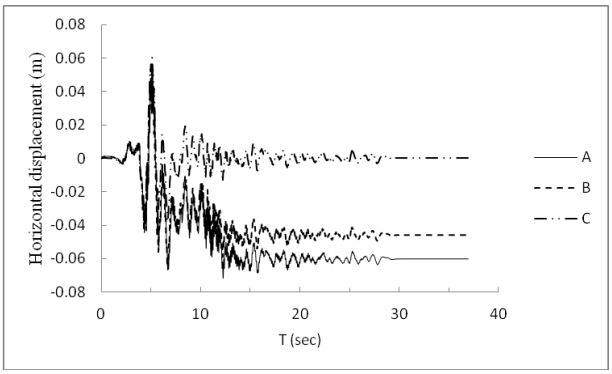

Figure 7-a: Lateral displacement induced in three points of the rock mass (Rock mass with horizontal discontinuities)

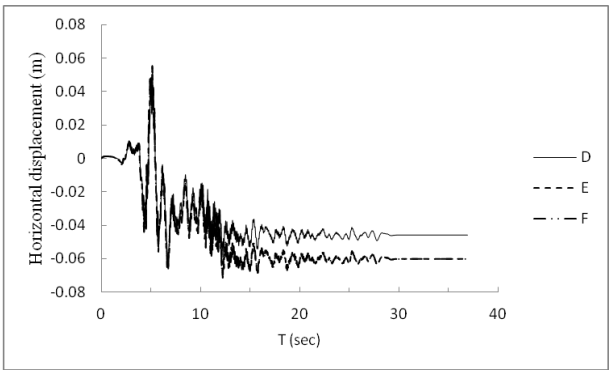

Figure 7-b: Lateral displacement induced at the top discontinuity (DEF) (Rock mass with horizontal discontinuities)

Figure 8 shows the profile of lateral displacement along the vertical section inside the area (Figure 3). At the beginning of loading (t = 2 s), there is a movement almost constant with depth, indicating a rigid block motion. At time t = 5 seconds, corresponding to the maximum loading, there is a shift of the upper part of the rock mass relative to the lower part. At the end of loading (t = 25 s), we note the return of the lower block to its original position (no lateral movement) and the presence of permanent sliding in the upper blocks.

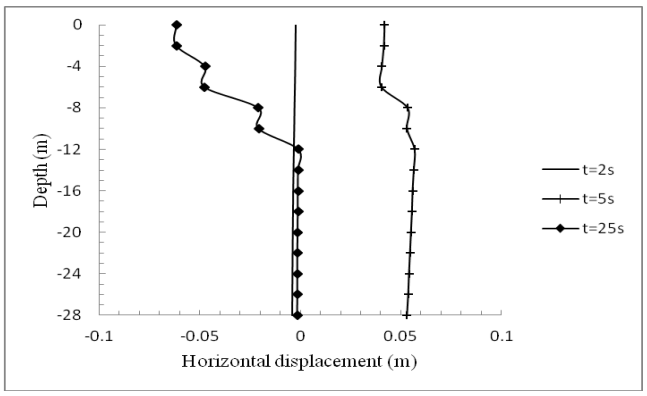

Figure 8: Lateral displacement along a vertical section (Rock mass with horizontal discontinuities)

Analysis of the seismic behavior of the rock mass - network of horizontal and vertical fractures

In this section, analyzes are performed considering the network of horizontal discontinuities (slight slope of 6.6 °) and a vertical discontinuity (slope of 79 °). Four plans of discontinuities are considered (three horizontal and one vertical) in the calculation (Figure 9) with the mechanical properties given in Table 2. A static calculation was performed to determine the initial constraints due to the weight of the mass.

Seismic Analysis

Figure 10 shows that the cliff is unstable. Between the second and third seconds from the start of loading, the points along discontinuities reach steady state and limit sliding movement is initiated failover and then a failing block is attenuated.

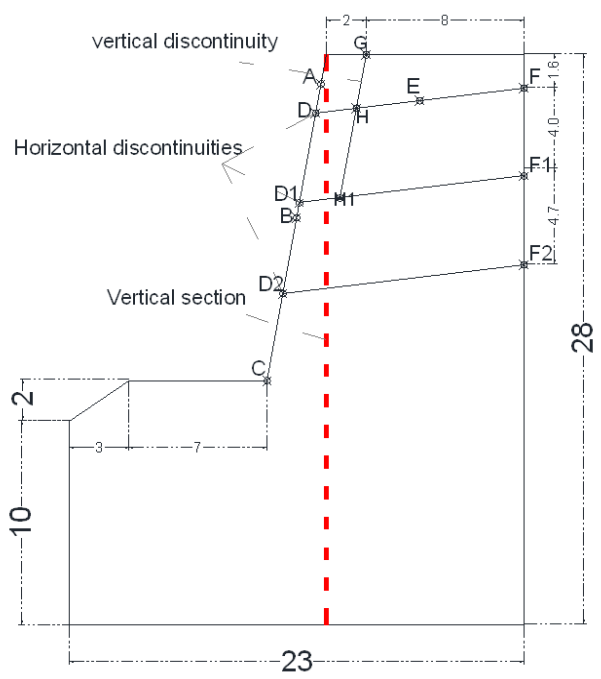

Figure 9: Domain considered in the modeling of the rock mass in jezzine in presence of horizontal and vertical discontinuities

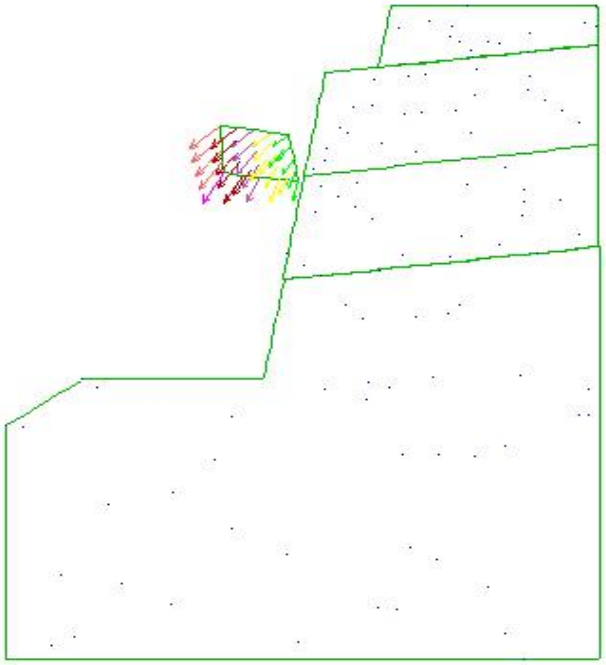

Figure 10: Displacement of the rock mass (after 10sec from the beginning of the seismic action)

Figure 11 shows the horizontal displacement of point A (top of the slope), this displacement increases slowly at the beginning of the earthquake, and between the second and third seconds, this increase accelerates and causes instability massif after 4 sec. After 3 seconds, the movement of the solid undergoes a major leap synonymous with instability.

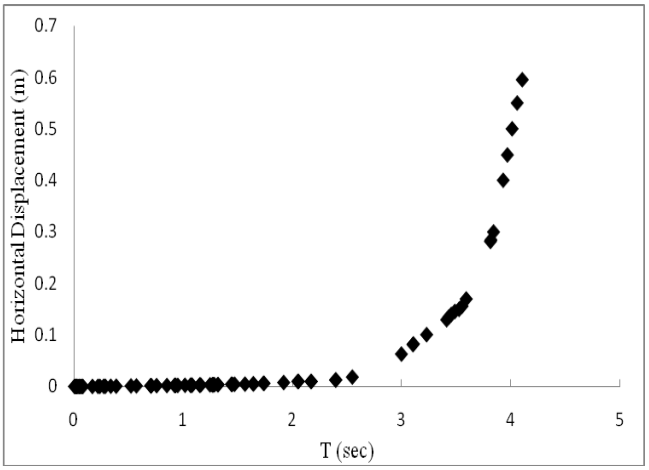

Figure 11: Displacement of the rock mass (after 10sec from the beginning of the seismic action)

Global Shearing-Resistant Reinforcement

In this section, we present the reinforcement of the unstable bloc using cables.

Cable Element Properties

The cable elements used in UDEC require several input parameters:

- cross-sectional area of cable;
- mass density for cable;
- elastic Young's modulus for cable;

- tensile yield strength [force] of the cable;
- compressive yield strength [force] of the cable;
- extensional failure strain for the cable;
- stiffness of the grout [force/cable length/displacement];
- cohesive capacity of the grout [force/cable length]; and
- spacing.

Results of the analysis

The analyzes were performed on the rock mass having horizontal and vertical fractures with the mechanical properties given in Table 3 for the cables.

Table 3: Mechanical properties of cables

Cross-sectional area of cable	0,18m^2
Mass density for cable	7,5 x 10^3 Kg/m^3
Extensional failure strain	1 x 10^{30}
Elastic Young's modulus (E)	98,6 GPa
Compressive yield strength	3 x 10^5 N
Tensile yield strength	81 x 10^{6}N (=450MPa x area)
Spacing	1 m
Stiffness of the grout	1,12 x 10^7 N/m/m
Cohesive capacity of the grout	1,75 x 10^5 N/m

As a first step, we analyzed the influence of the inclination of the cables on the response of the massif. Figure 12 shows the field and the network of horizontal and vertical discontinuities and five layers of cables. Figure 13 gives the results obtained with different inclinations. Note the instability of unreinforced and the massive reinforced with cables inclined at 45 ° and 90 °. The best performance is obtained with the horizontal cables.

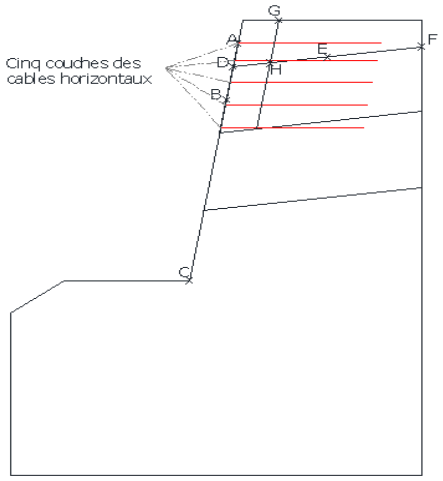

Figure 12: Vertical section showing the rock mass slope with all discontinuities and five horizontal layers of cables

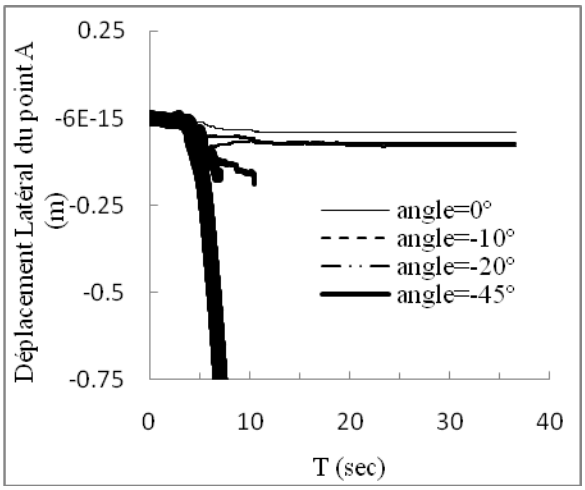

Figure 13: Horizontal displacement of point A with different inclinations of cables

Given below the results obtained with the horizontal reinforcement.

Figure 14 shows the horizontal displacements induced at points A, B and C of the cliff. At the beginning of loading, the displacements are identical in the three points. The maximum value of 6 cm is obtained to t = 5 sec. Then the shapes are significantly different with a significant gap between the point C (at the foot of the cliff) and points (A and B) at the top of the cliff. At the end of loading, there is a point C back to its original position and a permanent displacement of about 4 cm at points A and B. This trend shows that the seismic loading induced in the presence of horizontal discontinuities and vertical shifts in the permanent upper part of the rock mass which is similar to the case of absence of the horizontal layers of cables and vertical discontinuity.

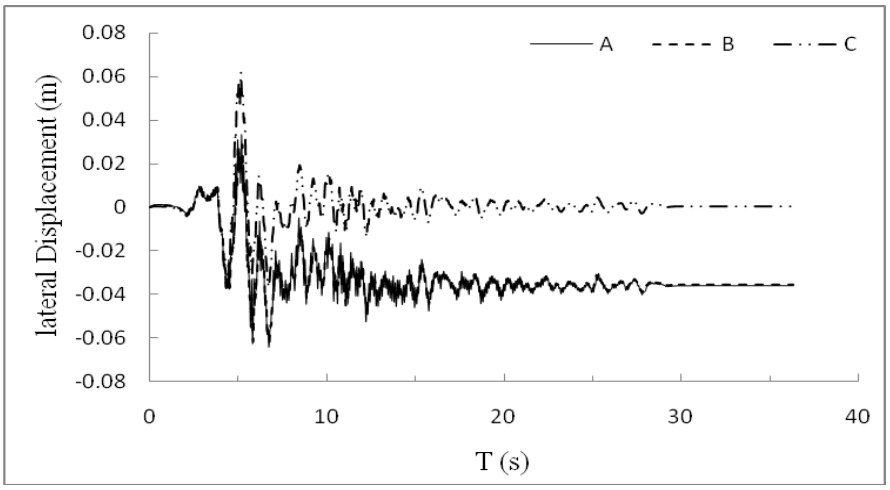

Figure 14: Lateral displacement induced by the seismic loading at 3 points of the rock mass

Analysis of the seismic behavior of the rock mass – in presence of water

Hydraulic properties

Table 4 shows the hydraulic parameter values used in our analysis.

Table 4: Values of hydraulic parameters used in the analysis

Parameters	Nomenclature	Units SI	value
a_{res}	Residual aperture	m	$2x10^{-4}$
$a_{zéro}$	Initial Aperture (at zero stress)	m	$5x10^{-4}$
ρ_w	Water density	kg/m^3	1000
μ_w	Dynamic viscosity of water	Pa.sec	10^{-3}
k_i	Permeability	1/Pa.sec	83.3

Analyzes are performed considering the network discontinuities quasi - horizontal (inclination 6.6°) and a near-vertical discontinuity (inclination 79°) with the reinforcement system to stabilize the rock mass. A static calculation showed that the massive sand is due to its own weight.

We imposed a pressure equal to 16.4; 56.2 and 103.11 kPa at points F, F_1 and F_2 (see Figure 10) respectively as boundary conditions with no water pressure at points D, D_1 and D_2.

Initial State – Static Calculation

Water in massive fractured may walk through the fractures. For higher values of normal stress, the surface area in contact between the walls is of the order of 40 to 70% of the total area of the walls [Bandis et al.].

Table 5 shows the values of the initial water pressure (before the application of seismic loading) at the ends of the joints. It may be noted that the hydrostatic pressure distribution, with a maximum at the point F_2 value of 100 kPa, the pressure is almost equal to the pressure imposed.

Table 5: Values (in kPa) of the initial water pressure at the ends of the joints

Case study	F	F_1	F_2	D	D_1	D_2
Rock Mass with horizontal discontinuities	16	54	100	0.52	1.8	3.3
Rock Mass with vertical discontinuities	16	54	100	0.19	1.7	3.3

Table 6 gives the values of the water flow in the joints. Note that the rates are very low. The maximum flow rate ($8x10^{-5}$ m^3/s) is observed in the lower discontinuity.

Table 6: Values (in 10^{-5} m^3/s) of water flow in joints

Case study	DH	HF	D_1H_1	H_1F_1	HH_1	D_2F_2
Rock Mass with horizontal discontinuities	2	2	5	5	-	8
Rock Mass with vertical discontinuities	_	2	7	5	2	8

Seismic Analysis

Table 7 summarizes the maximum changes in water pressure relative to its initial value at points D, D_1, F and F_1. Note that the seismic loading induced changes in water pressure which broadly follow the variations of seismic loading. The side F - F_1, the water pressure caused by seismic loading is lower than the initial water pressure. The ratio between the maximum variation of the water pressure and the initial pressure at point F is on the order of 0.6. On the coast D - D_2, the water pressure induced by seismic loading is higher than the initial water pressure. The ratio between the maximum variation of the water pressure and the initial pressure at point D, in presence of vertical discontinuities and reinforcement system, is of the order of 17.6.

Table 7: Maximal values of $\Delta P_w(t)/P_wi$

Case study	D	D_1	F	F_1
Rock Mass with horizontal discontinuities	9.6	3.71	0.6	0.29
Rock Mass with vertical discontinuities	17.6	20.6	0.6	0.42

Table 8 shows the maximum changes in water pressure reported in the normal stress at points D, D_1, F and F_1. Note that changes in the water pressure are low compared to the initial stress, especially at points D and D_1. This indicates a weak influence of the change in water pressure on the movement and stability of the rock mass.

Table 8: Maximal values of $\Delta P_w(t)/\sigma_ni$

Case study	D	D_1	F	F_1
Rock Mass with horizontal discontinuities	0.07	0.04	0.5	0.2
Rock Mass with vertical discontinuities	0.05	0.22	0.5	0.29

Table 9 shows the initial and maximum values of water flow at points D and D_1. The maximum values of this flow occurs when the seismic load peaked (at time t = 5 s). Note that the maximum flow induced by seismic loading is significantly higher than the initial rate. At point D, the ratio between the two rates reached 10.

Table 9: Initial and Maximal values of Water flow (in 10^{-2} m^3/sec)

Case study	D		D_1	
	Initial value	Maximal value	Initial value	Maximal value
Rock Mass with horizontal discontinuities	0.0027	0.02	0.006	0.05
Rock Mass with vertical discontinuities	0.0012	0.02	0.0072	0.16

Table 10 summarizes the maximum values of lateral displacement at points A and B in the absence and presence of water. Note that the presence of water has a significant influence on the move. For example, the displacement increases by 45% due to the presence of water.

Table 10: Maximum value of lateral displacement (in mm) at points A and B

Case study	Initial State – Dynamic Calculation	Lateral displacement in mm at points	
		A	B
Rock Mass with horizontal discontinuities	In absence of water	71.7	63.4
	In presence of water	94.0	92.2
Rock Mass with vertical discontinuities	In absence of water	64.4	61.9
	In presence of water	70.7	71.7

Table 11 shows the variations of the normal stress relative to its initial value at points D, D_1, F and F_1. Note that the seismic loading induces variations of the normal stress which broadly follow the variations of seismic loading. These variations are very large compared to the initial constraints.

Table 11: Maximal values of $\Delta\sigma_n(t)/\sigma_n i$

Case study	D	D_1	F	F_1
Rock Mass with horizontal discontinuities	13.85	20.35	65.2	21.15
Rock Mass with vertical discontinuities	54.93	20.35	65.2	21.15

Table 12 shows the variations of the shear stress relative to its initial value at points D, D_1, F and F_1. Note that the seismic loading induces important variations of the shear stress which broadly follow the variations of seismic loading. These variations are very large compared to the initial constraints.

Table 12: Maximal values of $\Delta\sigma_t(t)/\sigma_t i$

Case study	D	D_1	F	F_1
Rock Mass with horizontal discontinuities	26.1	9.3	149.06	14.2
Rock Mass with vertical discontinuities	90.4	37.7	149.06	19.97

CONCLUSIONS

In this paper, we analyzed the seismic response of a fractured rock mass which corresponds to a real case in Lebanon, the Jezzine. Static analysis, carried out to characterize the initial state in the solid, showed good stability of the rock mass under its own weight. Seismic analysis of massive with horizontal discontinuities shows a stability of the rock mass with a permanent displacement and a seismic analysis of massive with horizontal and vertical discontinuities shows instability of the rock mass. From the beginning of loading points along discontinuities reach steady state and limit sliding movement failover is initiated. There is also a stall of the upper block of the massif, where the need for the strengthening of unstable blocks by cables. This enhanced by a massive network of cables leads to a stabilization of solid with the appearance of a permanent shift in the upper part of the range.

And then we presented an analysis of the hydro-mechanical response of fractured rock masses to seismic loading. Computations were conducted using UDED Software with a full coupled hydro-mechanical analysis in the fractures (discontinuities).

Analyses showed that the seismic loading induced a significant change in the water pressure in the joints compared to the initial pressure, but that this variation has low impact on the rock mass response to the seismic loading.

REFERENCES

Abramson, L.W., Lee. T. S., Sharma, S., and Boyce, G. M. (1996) Slope stability and stabilization methods, *John Wiley & Sons, Inc,*.

Bandis S.C., Lumsden A.C. et Barton N.R (1983). Fundamentals of rock joints deformation. *Int. J. Rock Mech. Min. Sci. & Geomech. Abstr., vol. 20, no 6, pp. 249-268.*

Gentier S. "Morphologie et comportement hydromécanique d'une fracture naturelle dans le granite sous contrainte normale. Etude expérimentale et théorique". *Thèse de l'Université d'Orléans. Spécialté Mécanique des Roches, 2 vol., 637 pages, 1986]*

H. Sonmez, R. Ulusay, C. Gokceoglu (2000) A practical procedure for the back analysis of slope failures in closely jointed rock masses.

ITASCA. UDEC user's guide Ver. 5.0 (2011).

Jiu J. Jiao, Xu-Sheng Wang, Subhas Nandy (2005). Confined groundwater zone and slope instability in weathered igneous rocks in Hong Kong.

Luzia Fischer, Florian Amannb, Jeffrey R. Moore, Christian Huggel (2010). Assessment of periglacial slope stability for the 1988 Tschierva rock avalanche *(Piz Morteratsch, Switzerland).*

Morgenstern, N.R. (1970). The influence of groundwater on stability, *Procs. Of the first international conference on stability in open pit mining, pp. 65-81*.

Otter, J. R. H., A. C. Cassell and R. E. Hobbs (!966) "Dynamic Relaxation," *Proc. Inst. Civil Eng., 35, 633-665.*